

Simple Benzothiadiazole derivatives as buried interface materials towards efficient and stable n-i-p perovskite solar cells

Experimental Section

Material characterization equipment and instruments

The ^1H NMR, ^{19}F -NMR and ^{13}C NMR spectra were recorded on the Bruker Ascend 400 MHz spectrometer. High-resolution mass spectra were obtained with ThermoScientific™ Q-Exactive. Elemental analyses (EAs) of compounds were performed at Shenzhen University (Shenzhen, Guangdong, China).

Materials synthesis

The synthetic route of the target material is shown in Figure S1. 4,7-dibromobenzo[*c*][1,2,5]thiadiazole, 4,7-dibromo-5,6-difluorobenzo[*c*][1,2,5]thiadiazole, 4,7-dibromobenzo[*c*][1,2,5]thiadiazole-5,6-dicarbonitrile, 4,8-dibromobenzo[1,2-*c*:4,5-*c'*]bis([1,2,5]thiadiazole) and 4-(ethoxycarbonyl)phenylboronic acid were used as raw materials. All reagents and chemicals were commercially purchased and are used without further purification unless otherwise stated. Solvents were purified by standard methods and dried if necessary.

Synthesis of compound 1

4, 7-dibromo-2,1, 3-benzothiadiazole (100 mg, 0.34 mmol), 4- ethoxycarbonyl phenylboronic acid (165 mg, 0.85 mmol), Pd (PPh_3)₄ (43 mg, 0.034 mmol) were added to a round-bottom flask, K_2CO_3 (141 mg, 1.02 mmol), tetrahydrofuran (7 mL) and deionized water (1 mL) were heated to reflux reaction for 18 hours. After the reaction, it was cooled to room temperature, water and dichloromethane were added, extracted three times, the organic phase was combined, and dried with anhydrous sodium sulfate. The crude product was purified by column chromatography (silica gel, petroleum ether: dichloromethane =1:1 as the eluent) to afford a red solid in 92% yield (135 mg). ^1H NMR (400 MHz, CDCl_3) [ppm]: δ 8.25 (d, J = 8.3 Hz, 4H), 8.08 (d, J = 8.3 Hz, 4H), 7.88 (s, 2H), 4.46 (q, J = 7.1 Hz, 4H), 1.46 (t, J = 7.1 Hz, 6H). ^{13}C NMR (100 MHz, CDCl_3) [ppm]: δ 166.42, 153.84, 141.45, 132.94, 130.31, 129.85, 129.21, 128.46, 61.12, 14.38.

Synthesis of compound 2

The procedure is the same as compound 1. Yield: 71%.

^1H NMR (400 MHz, CDCl_3) [ppm]: δ 8.25 (d, J = 8.5 Hz, 4H), 7.92 (d, J = 8.3 Hz, 4H), 4.44 (q, J = 7.1 Hz, 4H), 1.44 (t, J = 7.1 Hz, 6H). ^{19}F NMR (376 MHz, CDCl_3): δ -132.03. ^{13}C NMR (100 MHz, CDCl_3) [ppm]: δ 166.15, 150.11, 150.08, 134.45, 131.07, 130.56, 129.68, 118.46, 61.24, 14.37.

Synthesis of compound 3

The procedure is the same as compound 1. Yield: 60%.

^1H NMR (400 MHz, CDCl_3) [ppm]: δ 8.27 (d, $J = 8.1$ Hz, 4H), 7.54 (d, $J = 8.1$ Hz, 4H), 4.45 (q, $J = 7.1$ Hz, 4H), 1.45 (t, $J = 7.1$ Hz, 6H)

Synthesis of compound 4

The procedure is the same as compound 1. Yield: 51%.

^1H NMR (400 MHz, CDCl_3) [ppm]: δ 8.29 (d, $J = 8.3$ Hz, 4H), 7.72 (d, $J = 8.3$ Hz, 4H), 4.46 (q, $J = 7.1$ Hz, 4H), 1.45 (t, $J = 7.1$ Hz, 6H). ^{13}C NMR (100 MHz, CDCl_3) [ppm]: δ 166.30, 150.59, 139.54, 138.09, 130.46, 130.41, 130.18, 113.07, 61.19, 14.40.

Synthesis of compound BT-BA

Compounds 1 (160 mg, 0.37 mmol), KOH (207 mg, 3.7 mmol), tetrahydrofuran (20 mL) and methanol (4 mL) were added to a round-bottom flask and heated to reflux for 24 hours. After the reaction, it was cooled to room temperature, all solvents were removed, followed by the addition of water and 2M dilute hydrochloric acid until the $\text{PH} < 7$ during which solid precipitation formed. The product was collected by filtration and washing quickly with methanol and ether. After dried in vacuum, 110 mg light green product was obtained in a yield of 79%.

^1H NMR (400 MHz, $\text{DMSO-}d_6$) [ppm]: δ 8.18 (d, $J = 8.5$ Hz, 4H), 8.13 (d, $J = 8.5$ Hz, 4H), 8.09 (s, 2H). ^{13}C NMR (100 MHz, $\text{DMSO-}d_6$) [ppm]: δ 167.59, 153.64, 141.25, 132.40, 130.94, 130.00, 129.81, 129.41. HRMS: $\text{C}_{20}\text{H}_{12}\text{N}_2\text{O}_4\text{S}$ calcd: 376.0518, found: 375.0443 [M-H]. Elemental Analysis: C, 63.82; H, 3.21; N, 7.44; S, 8.52, Found: C, 63.91; H, 3.32; N, 7.55; S, 8.59.

Synthesis of compound BTF-BA

The procedure is the same as the compound BT-BA. Yield: 66%.

^1H NMR (400 MHz, $\text{DMSO-}d_6$) [ppm]: δ 8.11 (d, $J = 8.1$ Hz, 4H), 7.81 (d, $J = 8.2$ Hz, 4H). ^{13}C NMR (100 MHz, $\text{DMSO-}d_6$) [ppm]: δ 167.60, 151.58, 138.26, 131.18, 130.71, 129.46, 123.95, 99.97. ^{19}F NMR (376 MHz, $\text{DMSO-}d_6$): δ -126.09. HRMS: $\text{C}_{20}\text{H}_{10}\text{F}_2\text{N}_2\text{O}_4\text{S}_2$ calcd: 412.0329, found: 411.0256 [M-H]. Elemental Analysis: C, 58.25; H, 2.44; N, 6.79; S, 7.77, Found: C, 59.01; H, 2.52; N, 6.65; S, 7.69.

Synthesis of compound BTCN-BA

The procedure is the same as the compound BT-BA. Yield: 70%.

^1H NMR (400 MHz, $\text{DMSO-}d_6$) [ppm]: δ 8.06 (d, $J = 8.1$ Hz, 4H), 7.42 (d, $J = 7.9$ Hz, 4H). ^{13}C NMR (100 MHz, $\text{DMSO-}d_6$) [ppm]: δ 167.56, 140.05, 136.59, 131.64, 130.58, 126.76, 117.53, 103.50. HRMS: $\text{C}_{22}\text{H}_{10}\text{N}_4\text{O}_4\text{S}$ calcd: 426.0423, found: 425.0116 [M-H]. Elemental Analysis: C, 61.97; H, 2.36; N, 13.14; S, 7.52, Found: C, 61.81; H, 2.53; N, 13.35; S, 7.63.

Synthesis of compound BBT-BA

The procedure is the same as the compound BT-BA. Yield: 90%.

^1H NMR (400 MHz, $\text{DMSO-}d_6$) [ppm]: δ 8.09 (d, $J = 8.0$ Hz, 4H), 7.64 (d, $J = 8.0$ Hz, 4H). ^{13}C NMR (100 MHz, $\text{DMSO-}d_6$) [ppm]: δ 167.83, 150.52, 140.94, 139.37, 131.30, 130.28, 129.95, 108.48. ^{13}C NMR (100 MHz, $\text{DMSO-}d_6$) [ppm]:

δ 167.83, 150.52, 140.94, 139.37, 131.30, 130.28, 129.95, 108.48. HRMS: $C_{20}H_{10}N_4O_4S_2$ calcd: 434.0143, found: 433.0043 [M-H]. Elemental Analysis: C, 55.29; H, 2.32; N, 12.90; S, 14.76, Found: C, 55.01; H, 2.52; N, 12.75; S, 14.69.

Device Preparation

Indium tin oxide (ITO, 20mm×20mm×11mm, <25 Ω per square) was successively ultrasonic in glass cleaning solution (15 minutes), pure water (15 minutes), acetone (15 minutes) and isopropyl alcohol (15 minutes), and blow-dried with an air gun, followed by UV treatment for 15 minutes. Then BTF-BA was dissolved in DMF to prepare the solution. In order to optimize the concentration, BTF-BA was configured with a series of concentration gradients ranging from 1mg/ml-15mg/ml and ultrasound was performed for 20min, and then deposited on ITO substrate by spin-coating at 2500rpm for 30s and annealed at 120° for 5min. BT-BA\BBT-BA\BTCN-BA\PCBM execute the same operation as above according to the optimal concentration (5mg/ml). In the preparation of TiO₂ ETL, FTO glass substrate is adopted because the preparation needs to be carried out at high temperatures. Then the FTO glass was blown dry after ultrasonic for 15min in glass cleaning solution, pure water, acetone and isopropyl alcohol, and UV treatment for 15 minutes. TiO₂ solution (1mlTiO₂+18ml tert-butyl alcohol) was then sprayed on the FTO substrate at 450 degrees to form TiO₂ ETL.

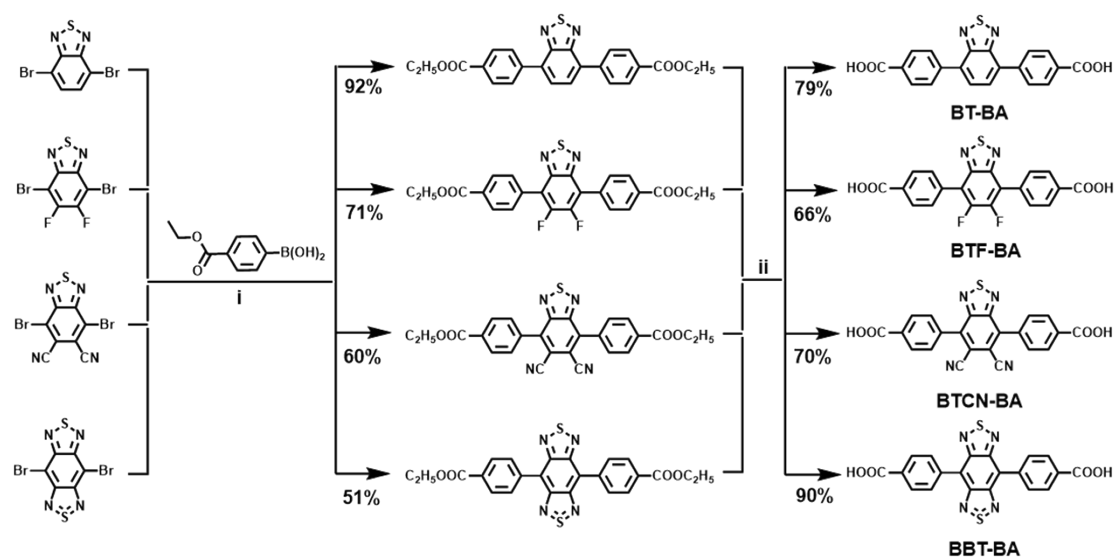
PSCs devices fabrication: for FA_{0.9}Cs_{0.07}MA_{0.03}Pb(I_{0.92}Br_{0.08})₃ precursor solution preparation, a mixture of MAI (6.4mg) FABr (13.5mg) CsI (24.6mg) MACl (31.9mg) PbBr₂ (39.6mg) FAI (190.4mg) Pbl₂ (591.2mg) was dissolved in 1 mL mixed solution of DMF and DMSO (volume ration of DMSO/DMF of 4:1). For hole transport material, 72.3mg spiro-OMeTAD was dissolved in 1ml CB with 42.2 ul Li-TFSI additives (520mg Li-TFSI dissolved in 1ml ACN and 1.64ml TBP). 50ul perovskite precursor solution was spin-coated in a two-step process at 1000 rpm for 10 s and 4000 rpm for 30 s, respectively. And in the last 10s of the second step, 260ul of EA is dropped onto the substrate as an antisolvent. The substrates were sequentially annealed at 100 °C for 40 min to form perovskite films. Then 50ul hole transport material spiro-OMeTAD was additives onto the perovskite at 3000rpm for 30s. Finally, an Ag electrode with 0.09 cm² active area (80mm) was deposited by thermal evaporation.

Samples Characterization

In order to exfoliate the perovskite from the bottom substrate, bisphenol A diglycidyl, octylamine and m-xyllylenedidamine are mixed with a mass ratio of 4:2:1, followed by sonication for 15 minutes. Poly (methyl methacrylate) (PMMA) was dissolved in chlorobenzene with a mass percentage of 32%. A thin layer of PMMA was coated on the perovskite film. Then a layer of resin-based film was coated on perovskite/PMMA by doctor blading. After drying in the air, the perovskite film can be easily stripped off completely with a scraper

and tweezer.

Top-views SEM images were obtained by using a SU-70 (Japan Hitachi Nake high-tech enterprise). The XRD pattern was carried out using Bruker-axs XRD with a Cu K α radiation source. The solar cells were measured using a solar simulator were measured using a Keithley 2400 Source Meter in combination with a solar simulator (Zolix Instruments) under AM 1.5 G illumination using a metal mask with an active area of 0.04 cm². The devices were characterized in a reverse scan mode (from 1.2 to -0.1 V at a step of around 0.02 V). Water contact angles on different ETLs were performed by using a video optical contact angle meter (KRUSS GmbH, DSA20) with 5s before shooting after water dripping. The UV-vis absorption spectra and transmittance spectra are measured by ultraviolet-visible (UV-Vis) spectroscopy (UV-1900). PL spectra were determined by a Fluorescence spectrophotometer (Horiba, Fluoromax-4) with an excitation at 460 nm. Electrochemical workstation (CHI 660) was taken to conduct EIS with a frequency range from 10 Hz to 800 kHz at an open-circuit voltage in dark conditions, C²-V spectra at a frequency of 10kHz with potential ranging from 0 V to 1.5 V, open-circuit voltage decay, I-V characteristics and transient photocurrent. AFM was measured by Cypher ES (Oxford Instruments Asylum Research) via contact mode with ASYELEC.01-R2 probe. Four-point probe tests were carried out by Lake Shore CRX-6.5K (Probe station for semiconductor device measurement). EQE was measured by a quantum efficiency measuring instrument (QE-R Enlitech). TGA was obtained on an Ultra-high temperature synchronous thermal analyzer (Setsys Evolution18).



Reagents and conditions: i) Pd(PPh₃)₄, K₂CO₃, THF, H₂O, reflux; ii) KOH, THF, MeOH, reflux.

Figure S1. Synthetic routes for BT-BA, BTF-BA, BTCN-BA and BBT-BA.

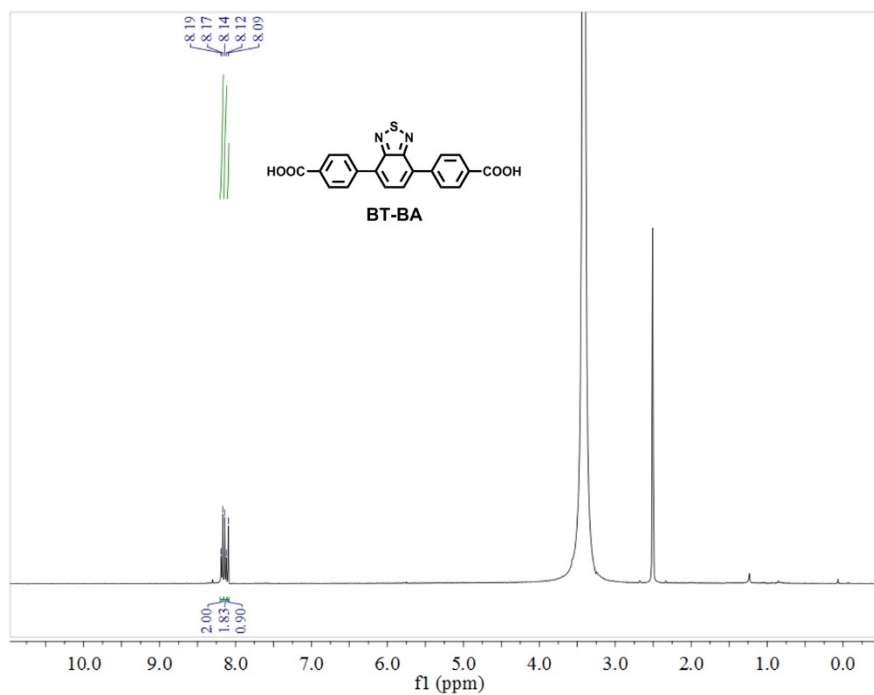


Figure S2. $^1\text{H-NMR}$ spectrum of BT-BA

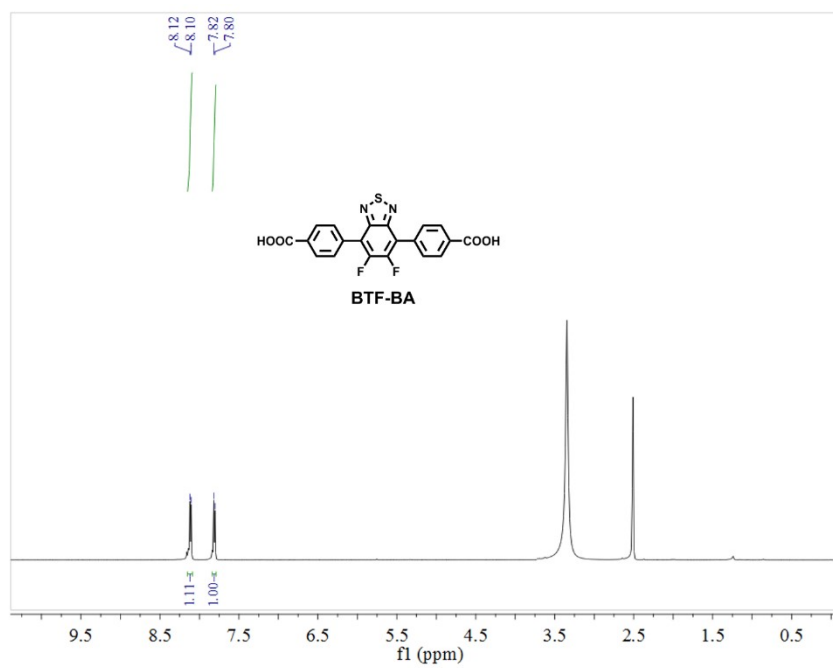


Figure S3. $^1\text{H-NMR}$ spectrum of BTF-BA

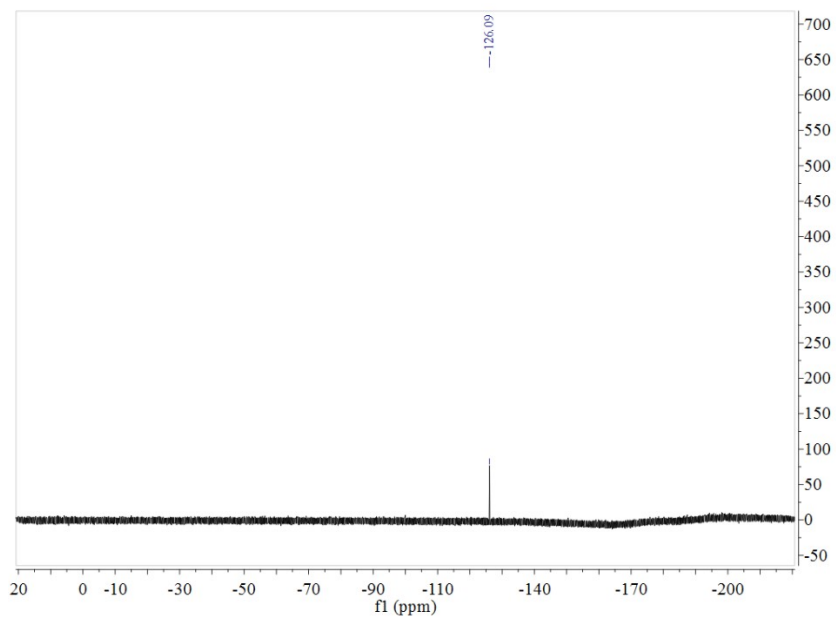


Figure S4. The ^{19}F -NMR spectrum for BTF-BA.

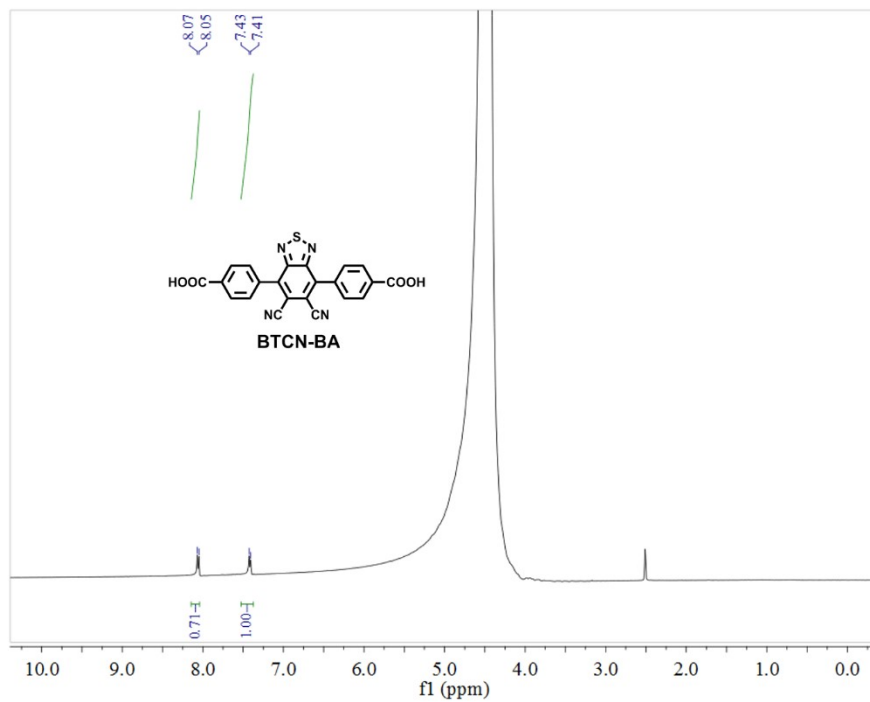


Figure S5. ^1H -NMR spectrum of BTCN-BA

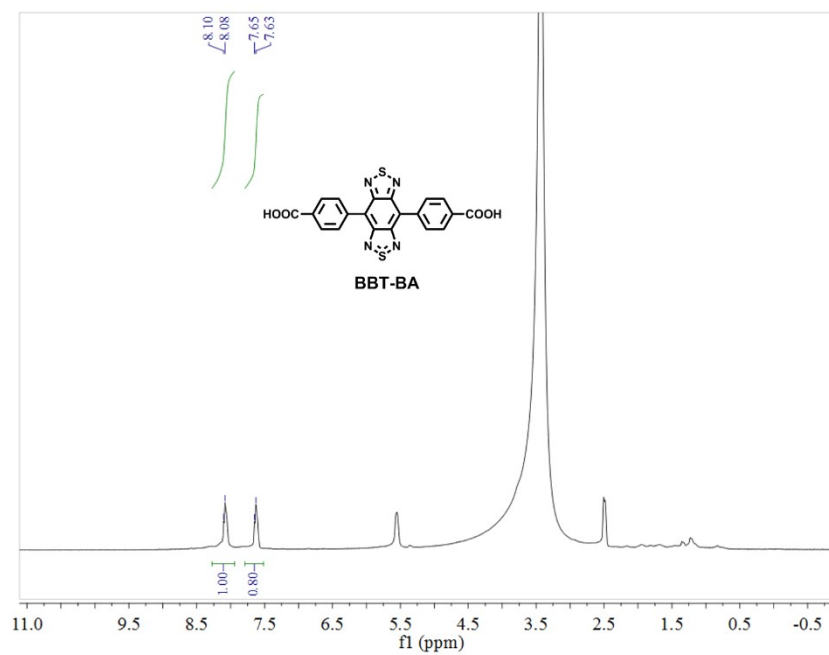


Figure S6. $^1\text{H-NMR}$ spectrum of BBT-BA

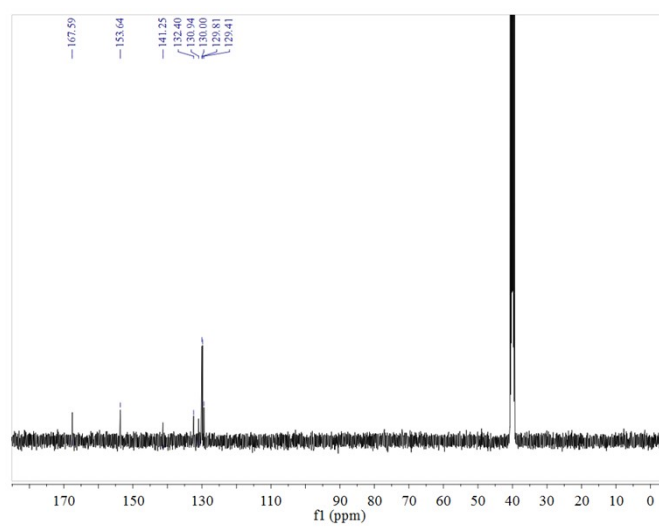


Figure S7. $^{13}\text{C-NMR}$ spectrum of BT-BA

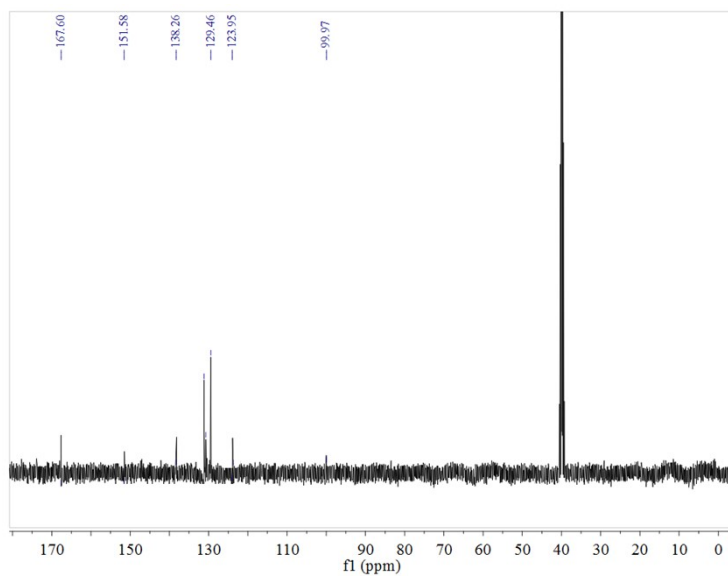


Figure S8. ^{13}C -NMR spectrum of BTF-BA

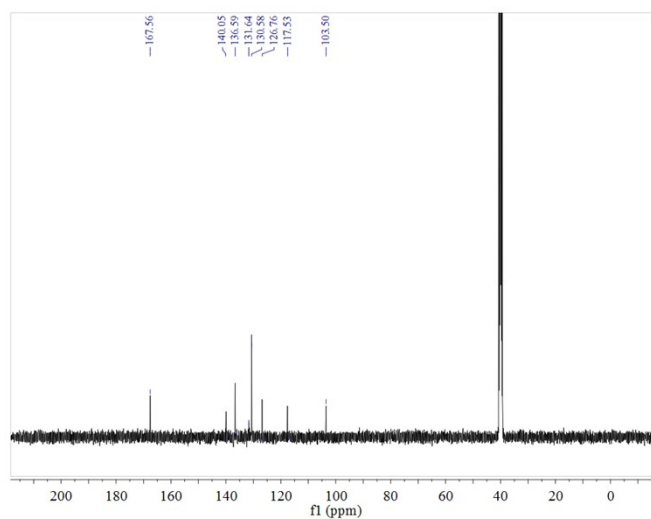


Figure S9. ^{13}C -NMR spectrum of BTCN-BA

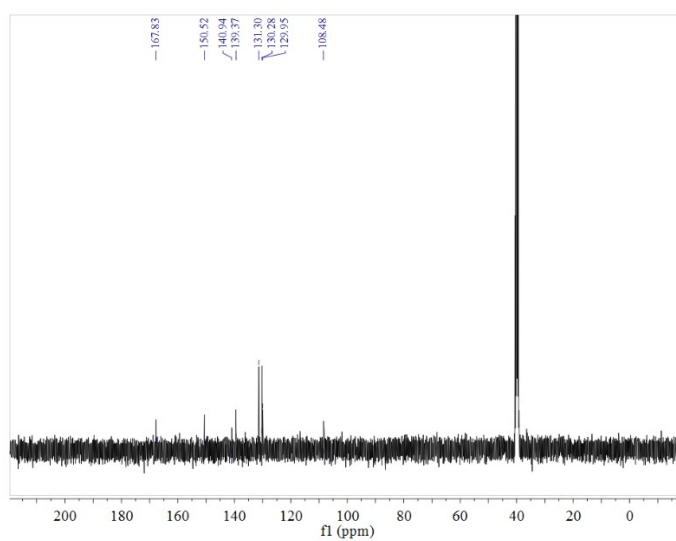


Figure S10. ^{13}C -NMR spectrum of BBT-BA

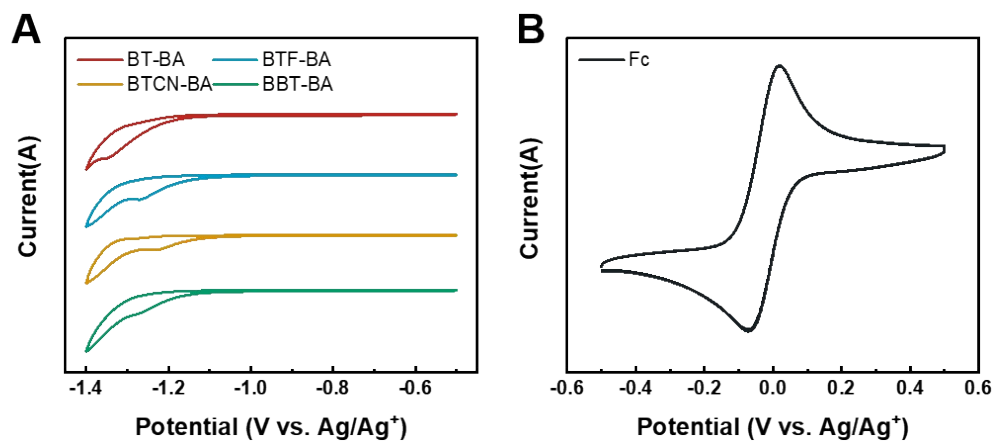


Figure S11. (A) Cyclic voltammograms of the BT series measured in 0.1 M tetrabutylammonium hexafluorophosphate solution in dichloromethane at a scan rate of 100 mV s⁻¹. (B) Cyclic Voltammograms of ferrocene as reference.

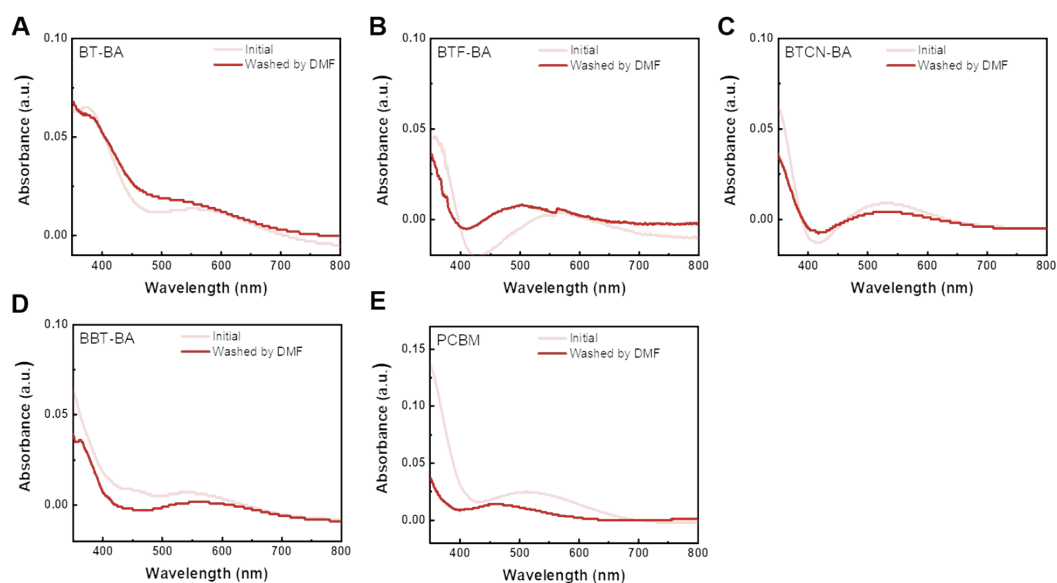


Figure S12. Variation of UV-vis absorption spectra of BT derivative and PCBM thin layers on ITO substrate upon DMF wash treatment.

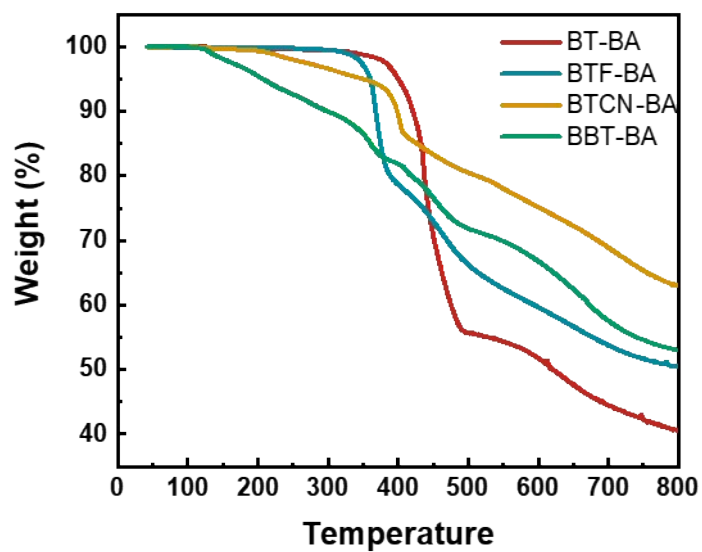


Figure S13. Thermogravimetric heating curve of BT derivative

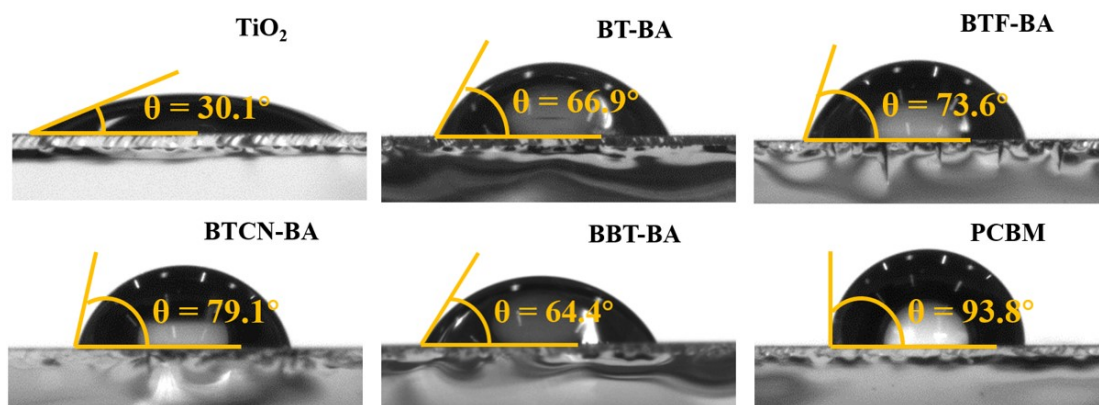


Figure S14. Contact angle measurements of different ETL

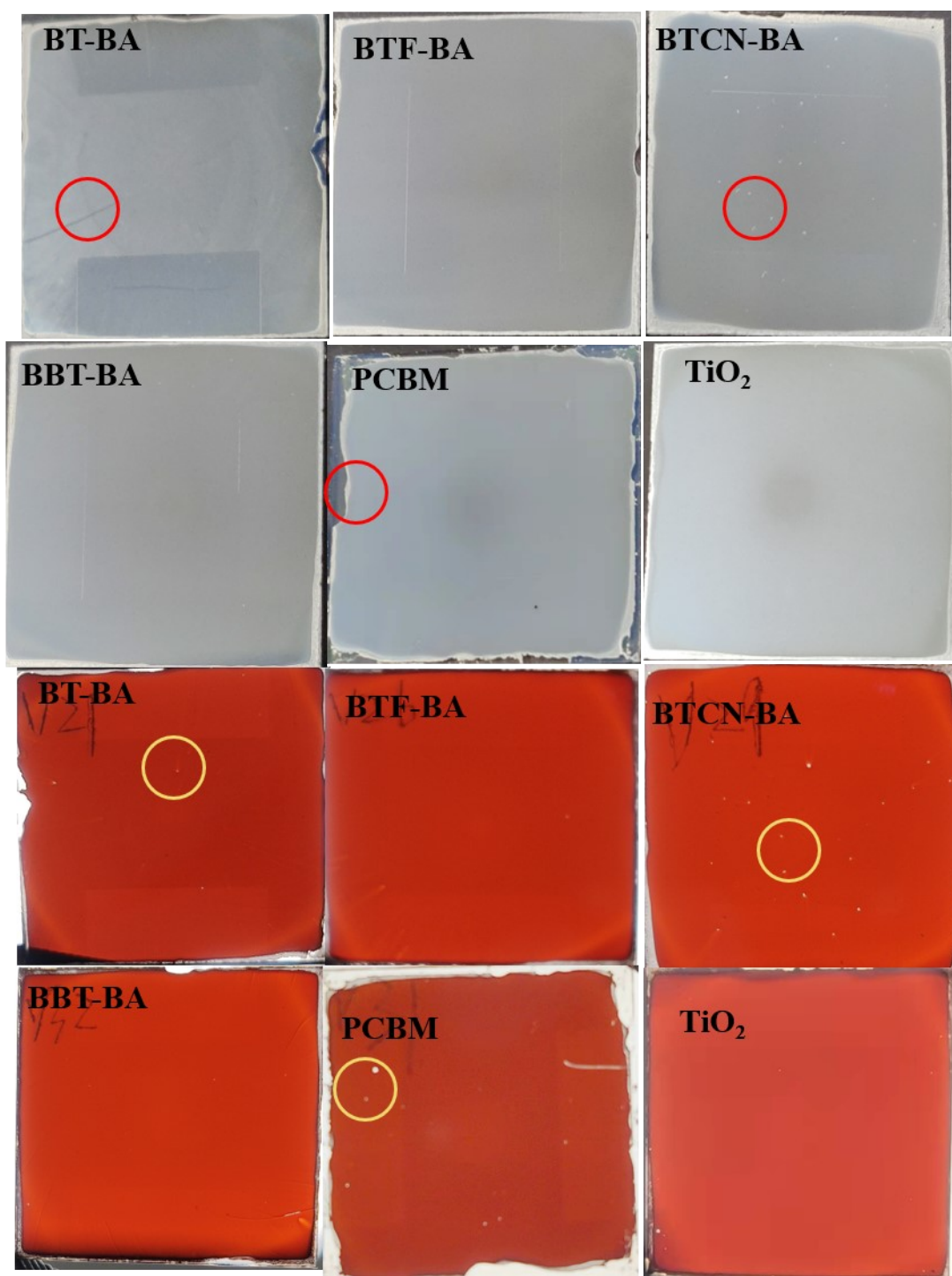


Figure S15. Images of perovskite films deposited on different ETMs from both front side (top two rows) and bottle side (last two rows)

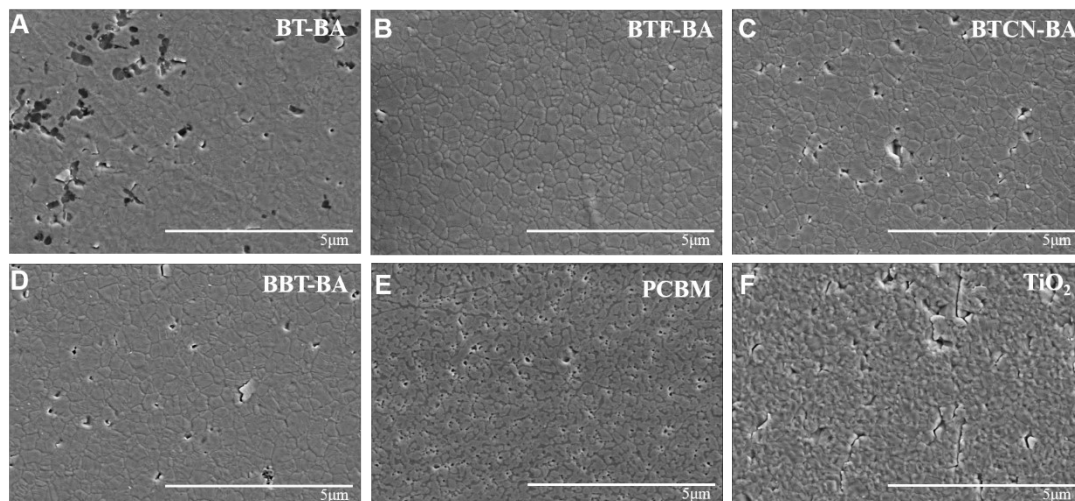


Figure S16. Top-view SEM images of perovskite films deposited on different ETL

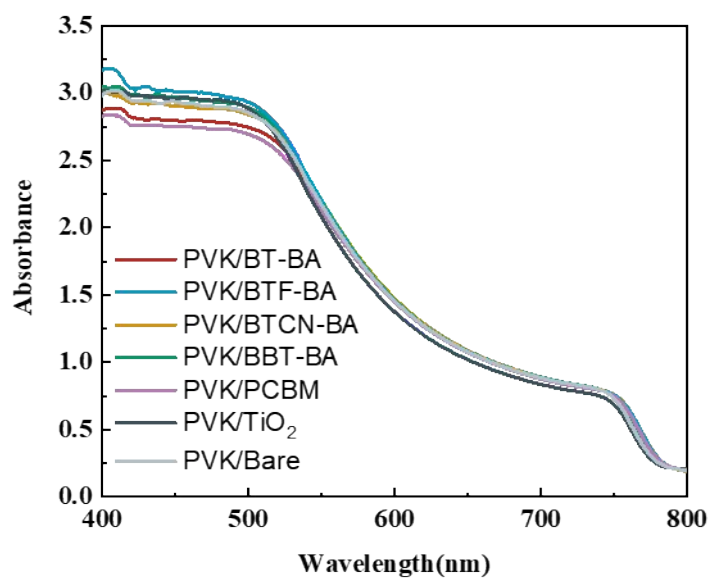


Figure S17. UV-vis absorption of perovskite film based on different ETLs.

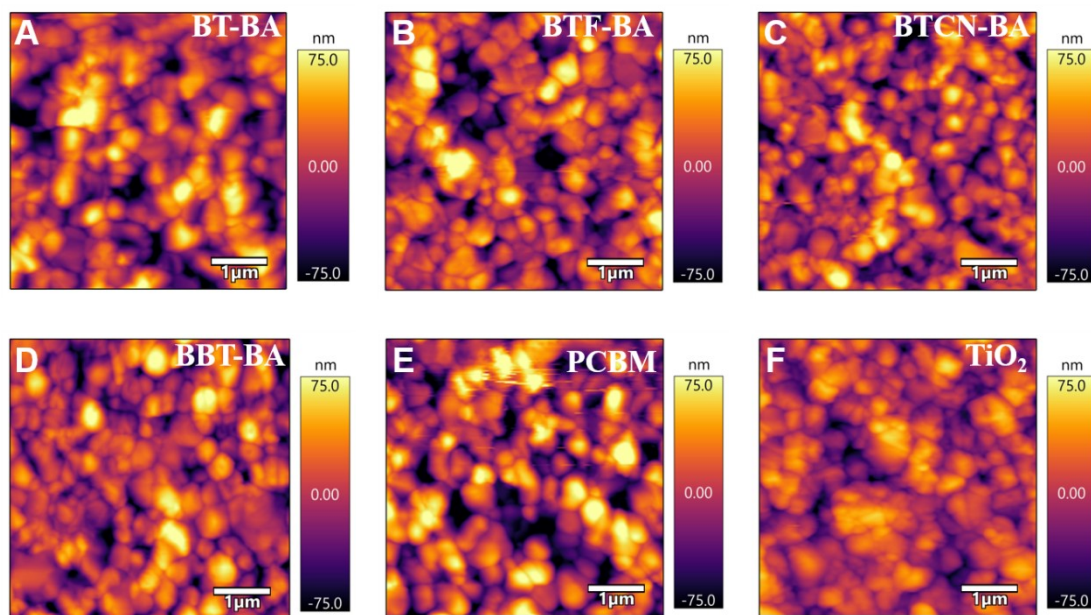


Figure S18. AFM morphological images of the ITO/ETL/ perovskite films, coated on (A) BT-BA, (B) BTF-BA, (C)BTCN-BA, (D)BBT-BA, (E)PCBM, (F)TiO₂, respectively.

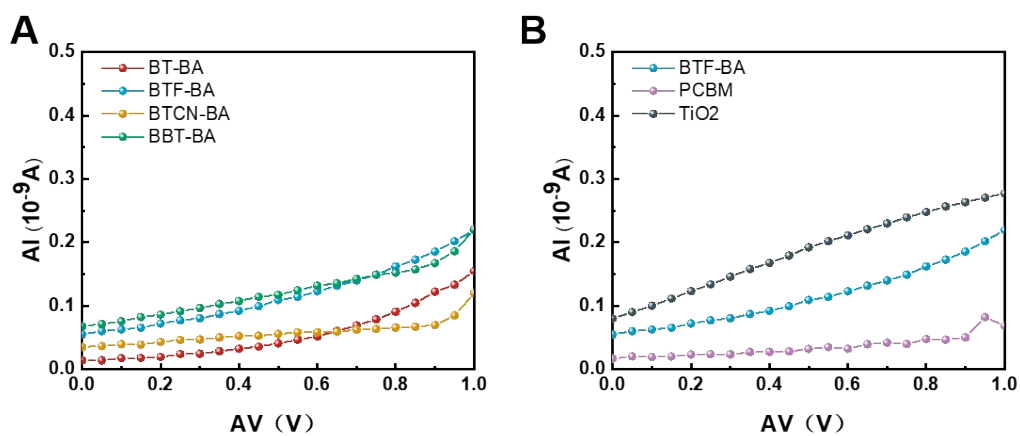


Figure S19. The resistivity of perovskite fabricated on different ETLs.

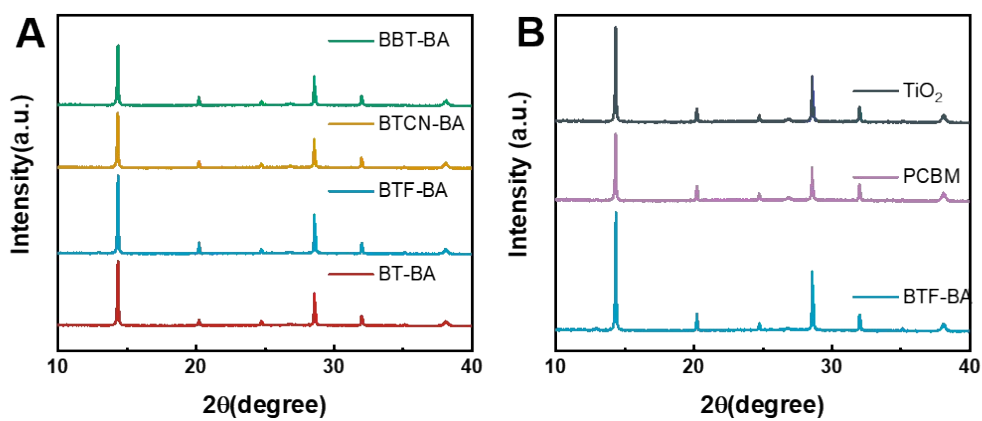


Figure S20. XRD pattern of perovskite films fabricated on different ETL.

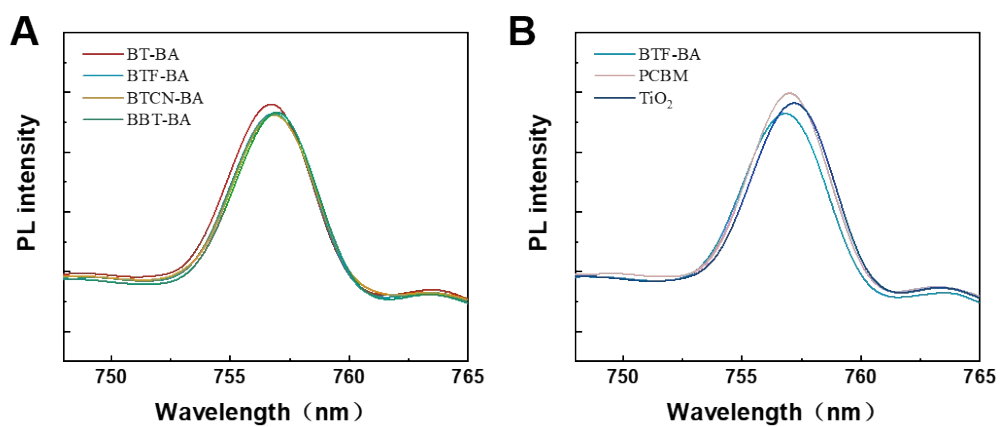


Figure S21. Steady-state photoluminescence (PL) of perovskite films fabricated on different ETMs from the substrate side.

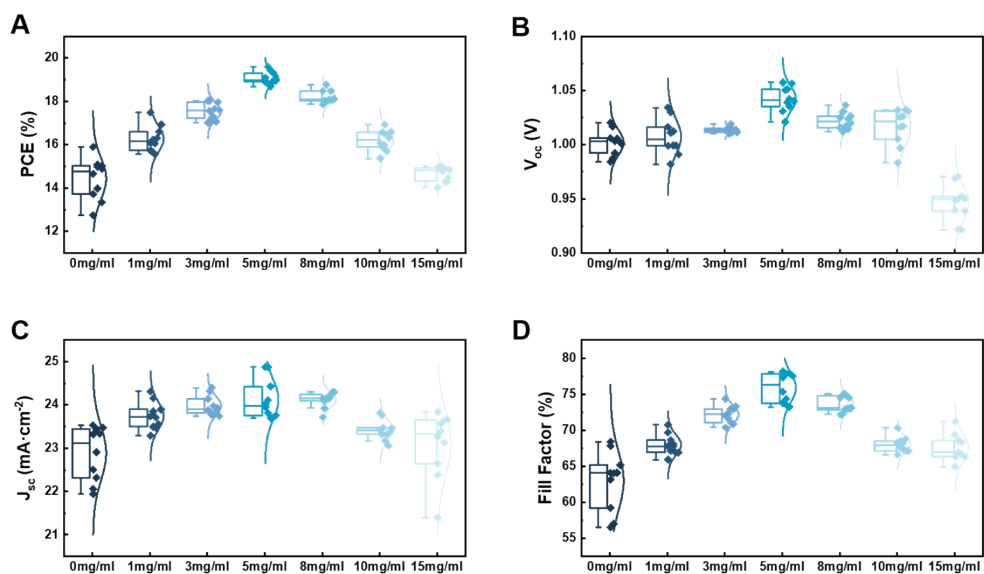


Figure S22. (A) PCE distribution of the PSCs based on BTF-BA with different concentrations. (B) V_{OC} distribution of the PSCs based on BTF-BA with different concentrations. (C) J_{SC} distribution of the PSCs based on BTF-BA with different concentrations. (D) FF distribution of the PSCs based on BTF-BA with different concentrations.

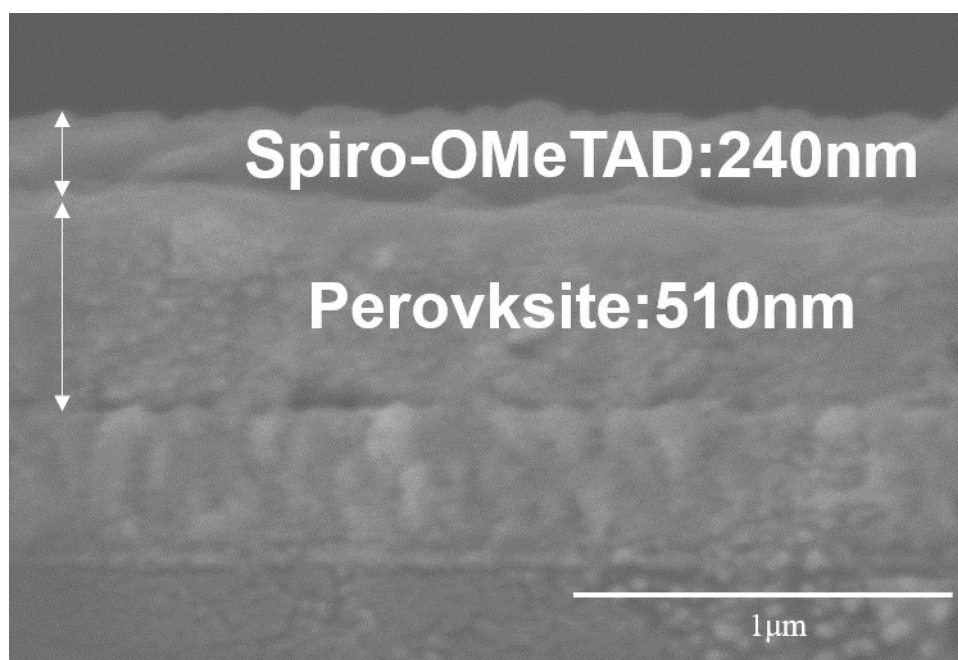


Figure S23. Cross-section SEM images of devices based on BTF-BA.

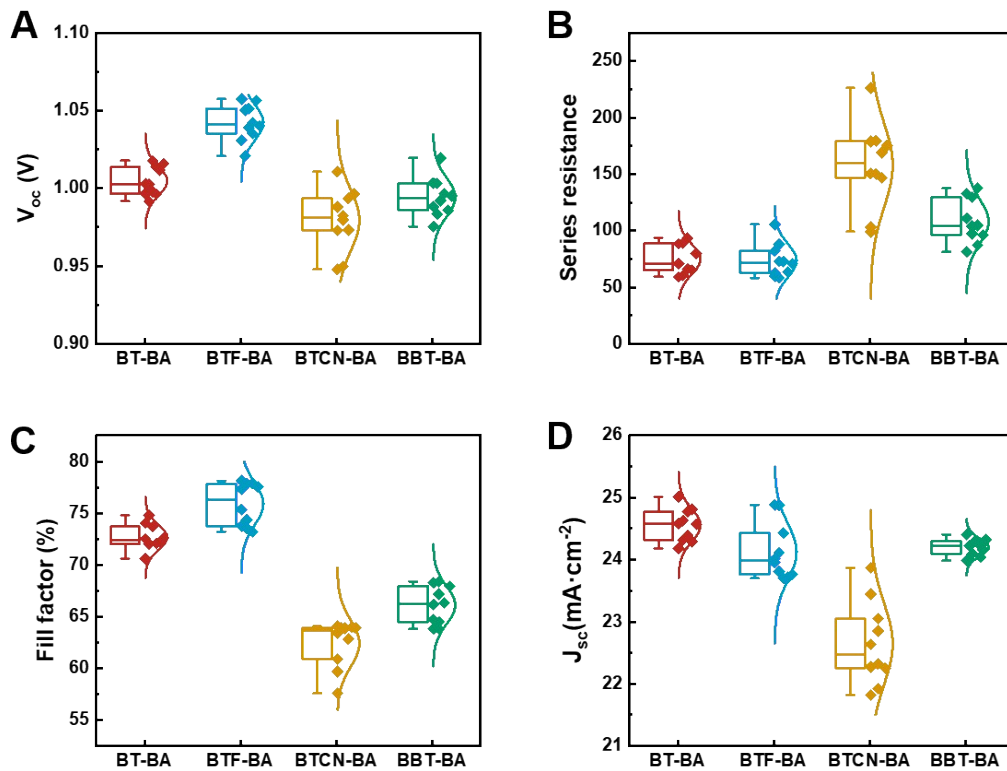


Figure S24. (A) V_{oc} distribution of the PSCs based on BT-BA, BTF-BA, BTCN-BA and BBT-BA. (B) Series resistance distribution of the PSCs based on BT-BA, BTF-BA, BTCN-BA and BBT-BA. (C) J_{sc} distribution of the PSCs based on BT-BA, BTF-BA, BTCN-BA and BBT-BA. (D) FF distribution of the PSCs based on BT-BA, BTF-BA, BTCN-BA and BBT-BA.

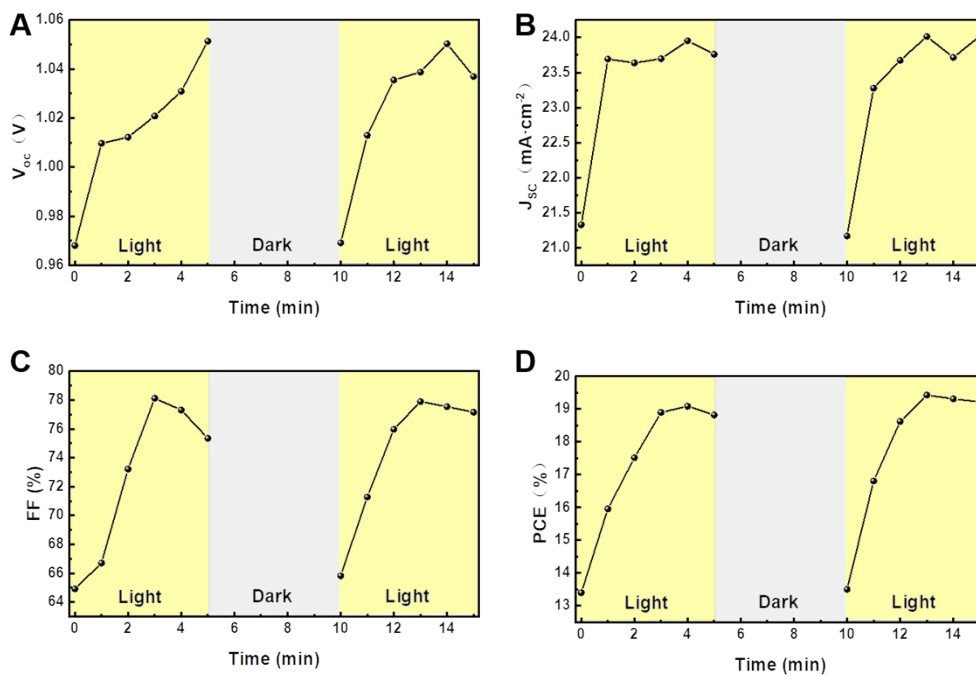


Figure S25. Evolution of (A) J_{sc} , (B) V_{oc} , (C) FF, and (D) PCE as a function of light soaking time.

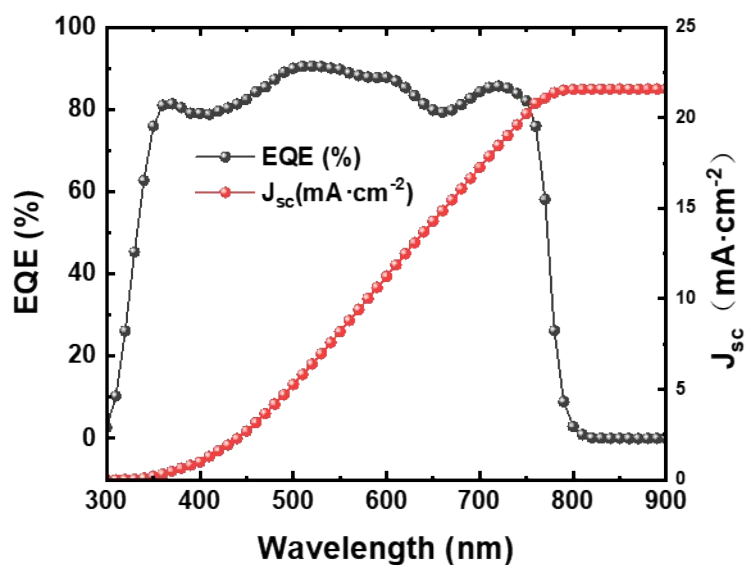


Figure S26. EQE of the champion devices based on BTF-BA

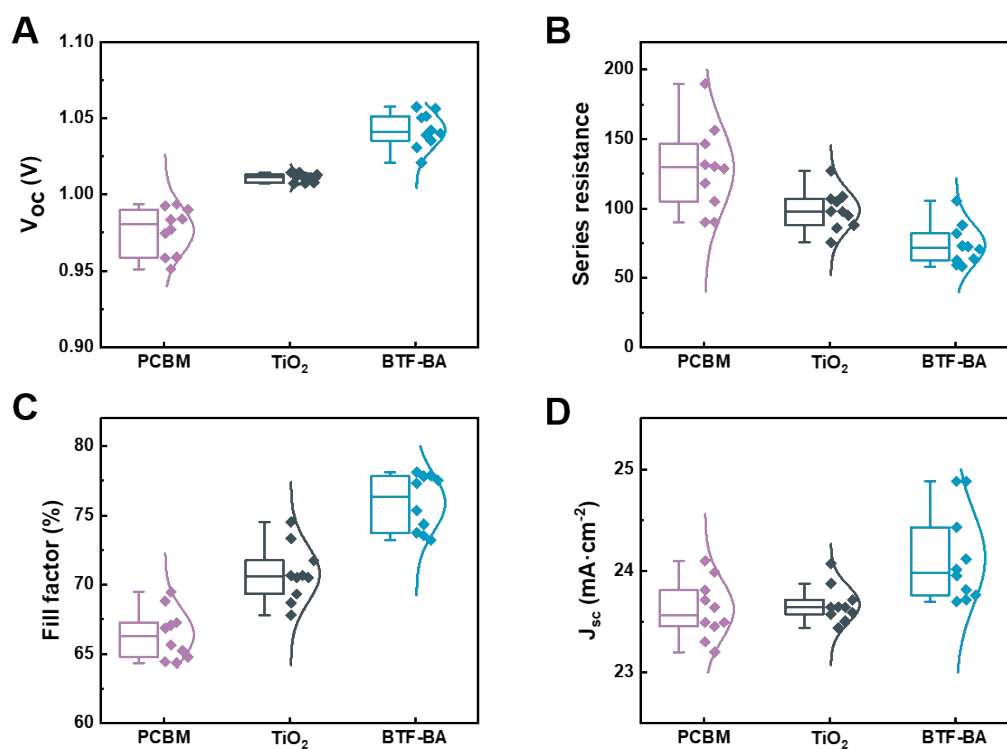


Figure S27. (A) V_{oc} distribution of the PSCs based on BTF-BA, TiO_2 and PCBM. (B) Series resistance distribution of the PSCs based on BTF-BA, TiO_2 and PCBM. (C) J_{sc} distribution of the PSCs based on BTF-BA, TiO_2 and PCBM. (D) FF distribution of the PSCs based on BTF-BA, TiO_2 and PCBM.

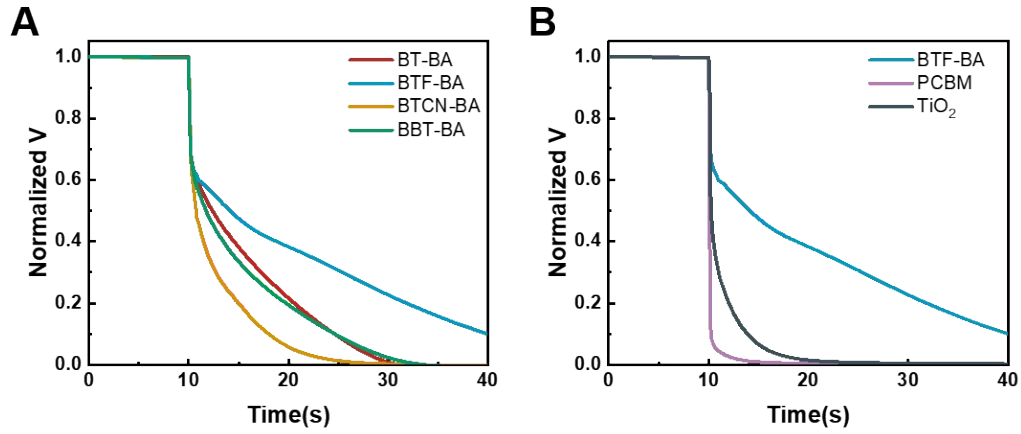


Figure S28. open-circuit voltage decay curves of PSCs based on different ETLs.

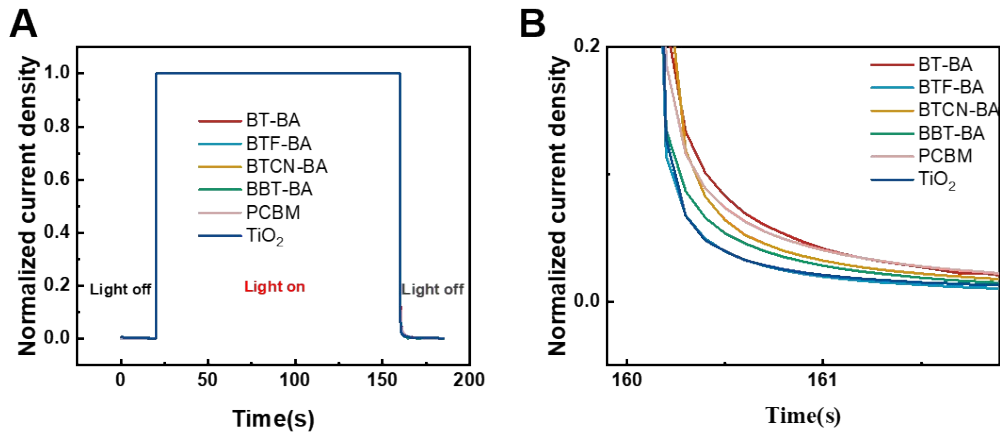


Figure S29. Photocurrent rising process on turning on and turning off the incident light for the devices based on different ETLs.

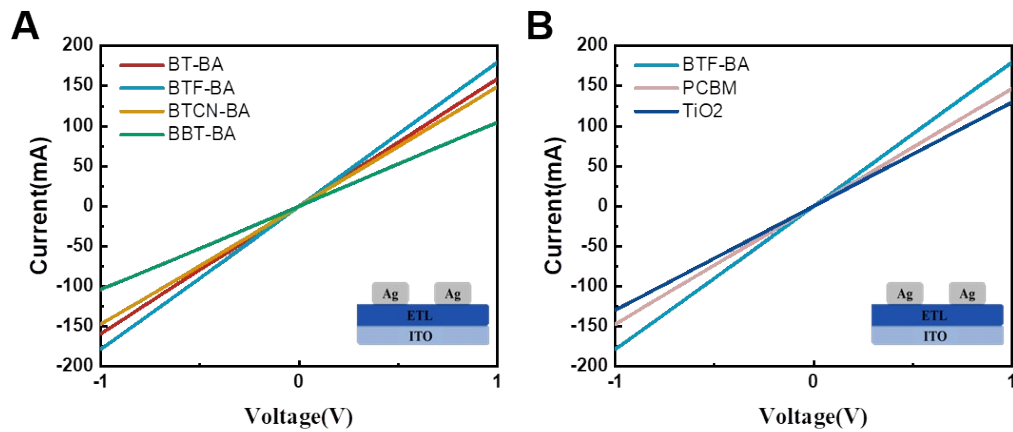


Figure S30. I - V characteristics of ITO/ETLs/Ag.

Table S1. The estimated cost for the synthesis of target molecules.

	Synthetic steps	Total Yield	Cost (US dollar per gram)
BT-BA	2	73%	10.6
BTF-BA	2	47%	112.5
BTCN-BA	2	42%	179.0
BBT-BA	2	45%	230.0
PCBM	-	-	393.27
TiO₂	-	-	43.45

Table S2. Optical and electrochemical properties of HTMs.

	$\lambda_{\text{onset}}(\text{nm})$	$E_g(\text{eV})$	$E_{\text{LUMO}}(\text{eV})$	$E_{\text{HOMO}}(\text{eV})$
BT-BA	430	2.88	-3.94	-6.82
BTF-BA	407	3.05	-3.99	-7.03
BTCN-BA	388	3.20	-4.02	-7.21
BBT-BA	490	2.53	-3.98	-6.51

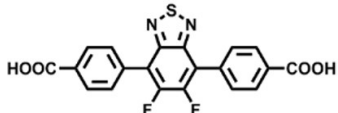
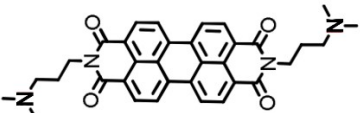
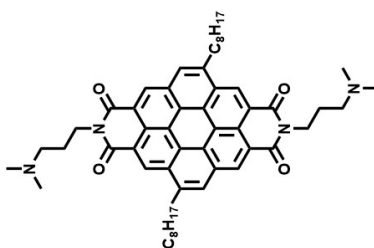
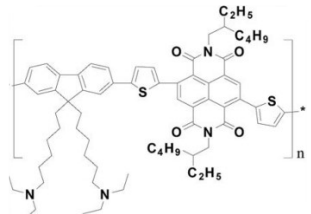


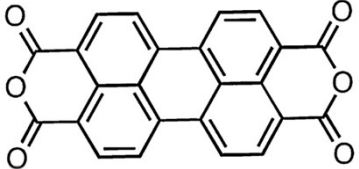
Table S3. The mean size of crystalline domains of perovskite films based on different ETLs.

	2θ	β	L
BT-BA	14.3435	0.0874	1.7359
BTF-BA	14.3435	0.0817	1.8571
BTCN-BA	14.3272	0.0889	1.6919
BBT-BA	14.3435	0.0880	1.7237
PCBM	14.3272	0.0826	1.8209
TiO ₂	14.3272	0.0866	1.7360

Table S4. Photovoltaic parameters for the champion PSCs based on BTF-BA with different concentrations.

	V _{oc} (V)	J _{sc} (mA·cm ⁻²)	FF(%)	PCE(%)
0mg/ml	1.01	23.32	67.80	15.90
1mg/ml	1.02	24.32	70.77	17.49
3mg/ml	1.01	23.93	74.31	18.03
5mg/ml	1.06	23.81	77.83	19.60
8mg/ml	1.04	24.14	75.03	18.77
10mg/ml	1.03	23.32	70.32	16.93
15mg/ml	0.95	23.57	66.93	14.99

Table S5. Comparison of non-fullerene organic electron transport materials in the literature for n-i-p structure perovskite solar cells.

Materials	Molecular structure	Device structure	PCE	reference
BTF-BA		ITO/BTF-BA/ Perovskite/spiro- OMeTAD/Ag	19.60	This work
N-PDI		FTO/N-PDI/ MAPbI _{3-x} Cl _x /spiro- OMeTAD/Au	17.66	J. Mater. Chem. A (2016) ¹
CDIN		ITO/PEIE/CDIN /CH ₃ NH ₃ PbI ₃ /spiro- OMeTAD/Ag	17.1	Advanced Materials (2016) ²
PFN-2TNDI		ITO/ PFN-2TNDI / MAPbI _{3-x} Cl _x /spiro- OMeTAD/Au	15.96	Chem Sci (2017) ³
FPDI		ITO/ FPDI / MA ₃ Bi ₂ I ₉ /spiro-OMeTAD/Ag	0.06	Journal of Alloys and Compounds (2018) ⁴
NDI-P		ITO/ NDI-P / MAPbI ₃ / spiro-OMeTAD/Au	16	Chem Commun (2019) ⁵
PTCDA		ITO/PTCDA/MAPbI ₃ / PTA /MoO ₃ /Ag	14.3	Synthetic Metals (2020) ⁶

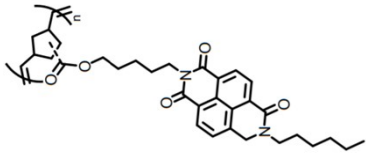
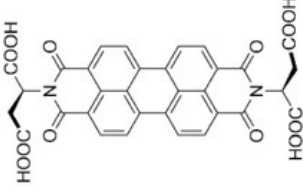
NDI-1		FTO/NDI-1/ FA _{0.79} Cs _{0.05} MA _{0.16} PbI _{2.49} Br _{0.51} /Spiro- OMeTAD/Au	14	Materials Chemistry Frontiers (2021) ⁷
PDI-LAS		ITO/ PDI-LAS / MAPbI ₃ / Spiro- OMeTAD /Au	18.77	Solar RRL (2021) ⁸

Table S6. The fitted parameters for EIS measurements acquired under dark based on different samples.

□	BT-BA	BTF-BA	BTCN-BA	BBT-BA	PCBM	TiO ₂
R_s	20.81	22.28	25.30	24.92	36.23	27.23
R_{rec}	218.70	432.30	155.80	226.10	65.52	290.10

Table S7. Value for the capacitance-voltage of the PSCs based on different ETLs.

□	BT-BA	BTF-BA	BTCN-BA	BBT-BA	PCBM	TiO ₂
V_{bi}	1.009	1.013	0.967	0.986	0.889	1.005

Reference

1. H. Zhang, L. Xue, J. Han, Y. Q. Fu, Y. Shen, Z. Zhang, Y. Li and M. Wang, *J. Mater. Chem. A*, 2016, **4**, 8724-8733.
2. Z. Zhu, J.-Q. Xu, C.-C. Chueh, H. Liu, Z. a. Li, X. Li, H. Chen and A. K. Y. Jen, *Adv. Mater.*, 2016, **28**, 10786-10793.
3. D. Li, C. Sun, H. Li, H. Shi, X. Shai, Q. Sun, J. Han, Y. Shen, H. L. Yip, F. Huang and M. Wang, *Chem. Sci.*, 2017, **8**, 4587-4594.
4. J. Huang, Z. Gu, X. Zhang, G. Wu and H. Chen, *J. Alloys Compd.*, 2018, **767**, 870-876.
5. L. Li, Y. Wu, E. Li, C. Shen, H. Zhang, X. Xu, G. Wu, M. Cai and W. H. Zhu, *Chem. Commun. (Camb.)*, 2019, **55**, 13239-13242.
6. S. Tsarev, S. Y. Luchkin, K. J. Stevenson and P. A. Troshin, *Synth. Met.*, 2020, **268**, 116497.
7. K. Al Kurdi, D. P. McCarthy, D. P. McMeekin, S. O. Furer, M.-H. Tremblay, S. Barlow, U. Bach and S. R. Marder, *Mater. Chem. Front.*, 2021, **5**, 450-457.
8. F. Ye, D. Zhang, X. Xu, H. Guo, S. Liu, S. Zhang, Y. Wu and W.-H. Zhu, *Sol. RRL*, 2021, **5**, 2000736.